Semi-insulating 4H-SiC lateral bulk acoustic wave resonators

Cite as: Appl. Phys. Lett. **118**, 114002 (2021); https://doi.org/10.1063/5.0045232 Submitted: 25 January 2021 . Accepted: 02 March 2021 . Published Online: 16 March 2021









View Onlin

ARTICLES YOU MAY BE INTERESTED IN

Carrier trapping and recombination at carbon defects in bulk GaN crystals grown by HVPE Applied Physics Letters 118, 112105 (2021); https://doi.org/10.1063/5.0040641

High n-type conductivity and carrier concentration in Si-implanted homoepitaxial AIN Applied Physics Letters 118, 112104 (2021); https://doi.org/10.1063/5.0042857

Measurement of the optical constants of monolayer MoS₂ via the photonic spin Hall effect Applied Physics Letters 118, 111104 (2021); https://doi.org/10.1063/5.0042422





Semi-insulating 4H-SiC lateral bulk acoustic wave resonators

Cite as: Appl. Phys. Lett. 118, 114002 (2021); doi: 10.1063/5.0045232 Submitted: 25 January 2021 · Accepted: 2 March 2021 · Published Online: 16 March 2021











B. Jiang, (i) N. P. Opondo, (ii) and S. A. Bhave (iii)

AFFILIATIONS

OxideMEMS Lab, Purdue University, West Lafayette, Indiana 47907, USA

a) Author to whom correspondence should be addressed: jiang561@purdue.edu

ABSTRACT

Silicon carbide (SiC) excels in its outstanding mechanical properties, which are widely studied in microelectromechanical systems. Recently, the mechanical tuning of color centers in 4H-SiC has been demonstrated, broadening its application in quantum spintronics. The strain generated in a mechanical resonator can be used to manipulate the quantum state of the color center qubit. This work reports a lateral overtone mechanical resonator fabricated from a semi-insulating bulk 4H-SiC wafer. An aluminum nitride piezoelectric transducer on SiC is used to drive the resonance. The resonator shows a series of modes with quality factors (Q) above 3000. An acoustic reflector positioned at the anchor shows a 22% improvement in Q at 300 MHz resonance and suppresses the overtone modes away from it. This monolithic SiC resonator allows optical access to the SiC color centers from both sides of the wafer, enabling a convenient setup in quantum measurements.

Published under license by AIP Publishing. https://doi.org/10.1063/5.0045232

Silicon carbide (SiC) is known for its hardness, elasticity at high temperatures, high thermal conductivity, and chemical inertness, making it suitable for the next-generation microelectromechanical systems (MEMS) components. Recently, the color centers in SiC, such as divacancies and silicon vacancies, have been demonstrated as viable platforms for quantum sensing and computation. In particular, researchers have been able to use surface acoustic waves (SAWs) in SiC resonators to control the spin states inside the acoustic cavity.² MEMS researchers have usually used SiC-on-Insulator (SiCOI) technology, which involves epitaxially grown SiC on an oxide layer. For example, 3C-SiC Lateral Overtone Bulk Acoustic Wave Resonator (LOBAR) devices developed by Gong et al.3 show outstanding resonance performance and are easy to fabricate at the wafer scale. However, semi-insulating (SI) 4H-SiC, a polytype that cannot be grown epitaxially, stands out as a unique candidate for its optical properties⁴ and its potential as the host for single quantum emitters.⁵

Recently, Lekavicius et al. introduced a diamond lamb wave resonator⁶ and created bright NV centers in it, a similar system to color centers in SiC. However, their devices are not integrated with a piezoelectric transducer and, therefore, cannot be mechanically actuated. We have previously fabricated cantilever resonators made from SI 4H-SiC⁷ resonating near 10 MHz and showed that the process preserves the fluorescence quality of the divacancies. The color center spin's mechanical Rabi frequency increases linearly with the frequency of the mechanical resonance, and so higher-frequency resonators are desired for fast quantum control. In this work, we report the development of 300 MHz acoustic wave resonators actuated by the aluminum nitride (AlN) piezoelectric layer on our SiC platform.

A 3D illustration for the device we made is shown in Fig. 1. We design the LOBAR devices based on a 200 μm thick 4H-SiC wafer. The LOBAR has an AlN transducer in the center, which has electrically alternating interdigitated transducer (IDT) fingers generating a laterally vibrating acoustic wave. The LOBAR generates overtone modes in the frequency spectrum, because of the SiC wings extending beyond the IDT-covered area on both sides. We also place an acoustic reflector, and an arc-shaped trench through the bulk wafer, centering at the LOBAR's anchor point. The leaking acoustic wave from the anchor incident on the trench will be reflected back into the resonator body, thus reducing the acoustic energy loss. For a reflector positioned at R_{ref} from the tether, the total wave propagating length is $2R_{ref}$. When $R_{ref} = \lambda/2 + n \cdot \lambda (n = 0, 1, 2, ...$ and λ is the acoustic wavelength), the highest Q values are achieved due to interference.

For quantum applications, when a laser is introduced to excite the color center spins in SiC, our device allows laser access to both surfaces of the SiC LOBAR, illustrated in Fig. 1. Compared with other MEMS resonators on SiC and diamond, ^{2,8,10,11} which are unreleased and allow only optical access from one side, our resonators would extend the sensing flexibility of spins. Optical access on one side will allow the sensing proximity to a measurand on the other, which is important in nanoscale sensing.¹²

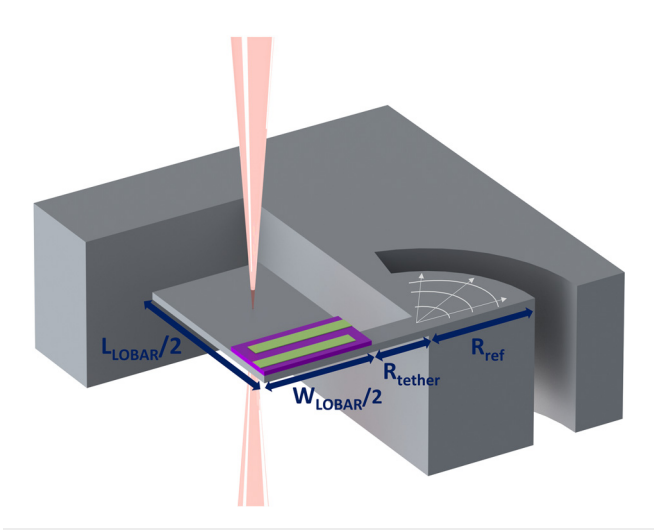


FIG. 1. 1/4th of the LOBAR resonator connected to the anchor area. The white lines indicate the mechanical wave leaking from the anchor, met by the reflector. The laser used for the quantum measurement can be applied from both the upper and the lower surface of the LOBAR's extending wings.

To find the appropriate design parameters, we performed a 2D COMSOL Multiphysics modal analysis based on the design shown in Fig. 2. Because of the simulation and fabrication limitations, we set the LOBAR length as $1600 \, \mu \text{m}$, the width as $300 \, \mu \text{m}$, and the thickness as $10 \, \mu \text{m}$, while R_{tether} as $90 \, \mu \text{m}$ and R_{ref} as $60 \, \mu \text{m}$. The distance between 2 IDT fingers is $20 \, \mu \text{m}$, leading to a resonance frequency around $300 \, \text{MHz}$.

We fabricate the SiC LOBAR devices from a 500- μ m-thick SI 4H-SiC wafer purchased from Cree Inc, with the resistivity larger than $1\times 10^6~\Omega$ cm. The wafer is thinned down to 200 μ m by chemical mechanical polishing (CMP). The detailed process after thinning is shown in Fig. 3(a): (1)–(3) a piezoelectric stack consisting of 1 μ m AlN sandwiched between the 100 nm molybdenum (Mo) layer is deposited by OEM Group, Inc. Optical lithography and dry etch are performed to define the piezoelectric transducers. (4) The key fabrication step involves a dual-mask followed by front-backside etch, enabling a wafer-scale dry release of the LOBARs. For the hardmask of the SiC

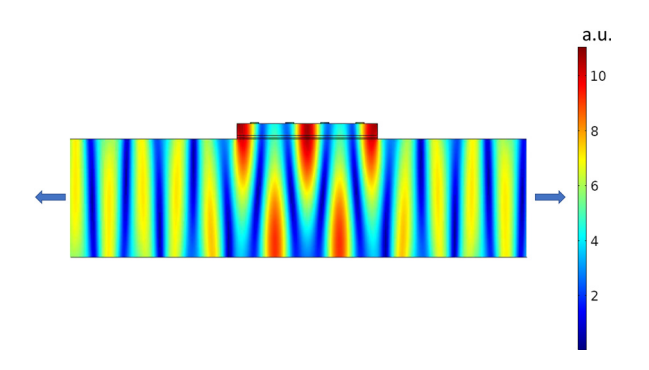


FIG. 2. Mode shape of the LOBAR device, shown as the displacement in COMSOL simulation. The IDT fingers in the center region create the alternative mechanical vibration to both sides.

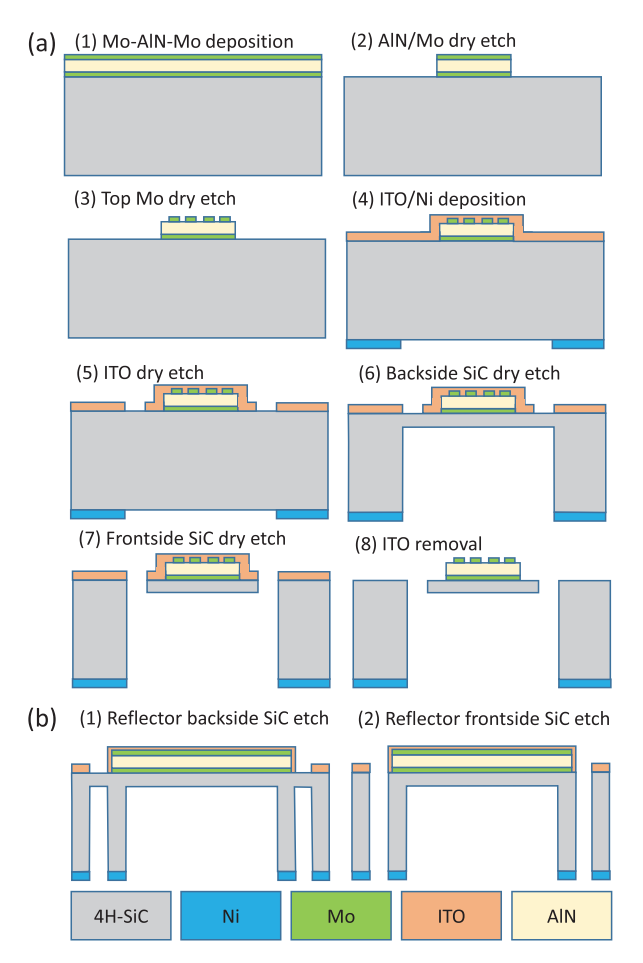


FIG. 3. (a) Fabrication process of the SiC LOBAR resonator. The cross section is along the longitudinal direction of the LOBAR. (b) Fabrication of the reflectors. The figures correspond to steps (6) and (7) in (a). The cross section is along the transverse direction of the LOBAR. Compared with the previous acoustic reflectors, which were only defined by frontside etch, our front-backside etch allows a reflector through the whole wafer thickness. It may be used in future developments in anchor loss reduction.

etch, we deposit 4- μ m-thick Nickel (Ni) on the backside.⁷ At the same time, we use electron beam evaporation to form an indium tin oxide (ITO) thin layer (600 nm) as the etch mask for the frontside of SiC since it can be dissolved by wet etch without damaging the metal electrodes. (5) The ITO layer is patterned by photoresist and then etched by Cl₂ based plasma, to define the release window for LOBARs. (6) From the backside, SiC is dry etched with SF₆ and Ar plasma. The etch rate is about 15 μ m per hour. The etch is stopped when it reaches 190 μ m, leaving a 10 μ m SiC membrane. (7) Turning over the wafer, we perform another dry etch on the frontside for $10 \,\mu m$ until the LOBAR device is released. (8) Finally, we dissolve the ITO with 1:5 = HCl:H₂O diluted hydrochloric acid and leave the backside Ni mask on as it does not affect our measurement. The acid does not attack the AlN transducer stack. Concurrently, a through wafer 200 μ m acoustic reflector is defined using the frontside 10 and 190 μ m deep etches, shown in Fig. 3(b).

The final devices are inspected using a Hitachi S-4800 Field Emission SEM. The images are shown in Fig. 4. The SiC LOBAR is released using our front-backside etch. One challenge in the fabrication is that the main LOBAR release window is much larger than the reflector, resulting in different etch rates in these two regions. When the backside etch reaches 190 μ m in the LOBAR area, the reflector etch on the backside is shallower. We overcome the issue by an overetch on the frontside with an ITO hardmask. ITO shows a selectivity of 1:50 over SiC and survives the extensive etch on the frontside. Fig. 4(b) shows the piezoelectric transducer defined on top of SiC LOBAR. Even though the dry etch of AlN with BCl₃ stops on the SiC layer, it leaves a rough surface due to heavy Cl⁻ ion bombardment.

The resonators are characterized on a Cascade Microtech 11971B Probe Station with a Keysight N5230A PNA-L Network Analyzer and 2 Cascade Microtech ACP40 GSG probes at room temperature and under atmosphere conditions. In Fig. 5, we compare the transmission measurements of LOBARs with and without the reflectors. The Q values are calculated using the Lorentzian peak fitting method. The piezoelectric transducer couples to multiple overtones in the resonator. We define the target mode of the LOBAR as the mode with maximum coupling with the transducer. We realize a 22% improvement in Q in the target LOBAR mode with the reflector. In Fig. 5(c), the LOBAR with the reflector has increased Q values around 300 MHz, while the Q values of other overtone modes quickly decline and vanish below the measurement noise floor outside a 100 MHz wide range. Meanwhile, the LOBAR without the reflector displays lower Q values across a wider frequency spectrum.

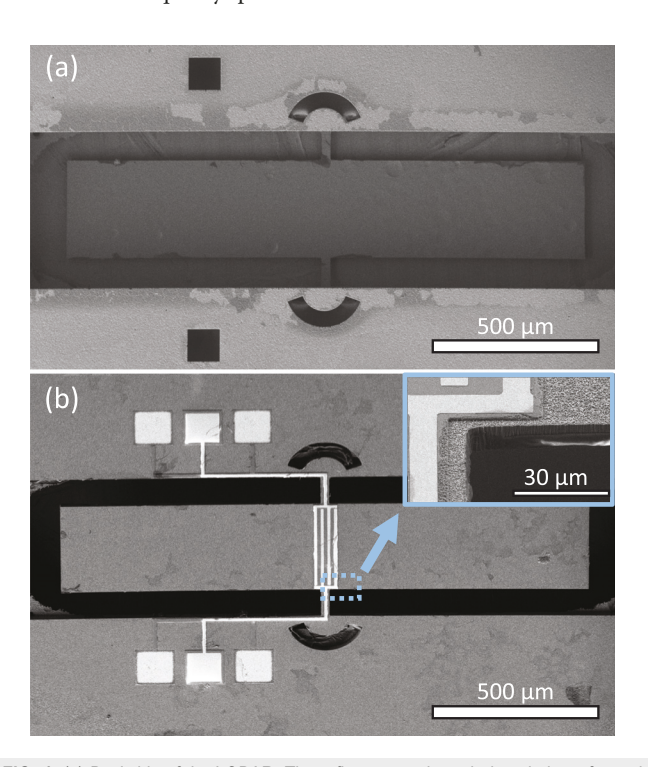


FIG. 4. (a) Backside of the LOBAR. The reflectors go through the whole wafer and have openings on both sides of the wafer. The LOBAR is 1600 $\mu \rm m$ long and 300 $\mu \rm m$ wide. (b) Frontside of a released LOBAR. The enlarged picture shows SiC surface damage during the AIN etch.

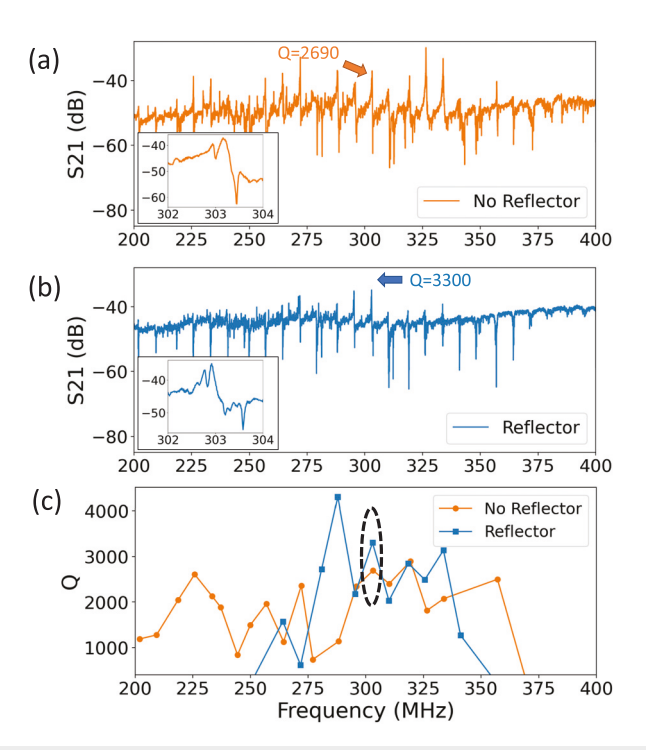


FIG. 5. 2-port transmission measurements of (a) LOBAR without the reflector and (b) LOBAR with the reflector, $R_{ref}=1.5\lambda$. The reflector is frequency-sensitive, suppressing the resonances away from 300 MHz. (c) Q measured in both devices' overtone modes. The circled two modes are the marked ones and shown in insets in (a) and (b), respectively.

As it is discussed in Fig. 1, for a designed $R_{ref}=60\mu m$, Q is maximized when the wavelength $\lambda=40~\mu m$ and n=1. With an acoustic velocity of 12500 m/s, ¹⁴ this wavelength corresponds to a frequency of 300 MHz in 4H SiC. Other modes are affected by the miss-matched interference and suffer a Q loss. A LOBAR has multiple modes with similar Q values and piezoelectric coupling. Appropriate design and positioning of the acoustic reflector enhance the target mode and attenuate the adjacent modes' Q values. This Q boost will enhance the strain-spin coupling in the color center applications in SiC. Our design will also simplify spur-free RF LOBAR oscillators. ¹⁵

The SI 4H-SiC resonators' Q values are similar to those of the previous 3 C-SiC LOBARs³ and the SCHBAR in diamond,¹¹ but still lower than the LOBARs made by Ziaei-Moayyed *et al.*¹⁶ Future fabrication improvement to increase the Q value will include reducing the surface roughness in AlN etch on the frontside and reducing the dimples, and improving the etch depth uniformity on the backside and increasing the sidewall smoothness.

In conclusion, we have introduced a monolithic high-frequency lateral bulk acoustic wave resonator based on SI 4H-SiC and improved its mechanical performance by a reflector design. The front-backside etch process provides unique flexibility to produce other types of resonators. ^{17–20} In the future, we shall explore the mechanical coupling to the color centers using our devices and study the effect of a laterally vibrating acoustic wave on the quantum system. Furthermore, since no other substrate material is needed and the optical accessibility is on both sides, we can combine this process with the development of 2D

material on SiC²¹ and study the acoustic effect on the interface between the two materials.

This work was conducted at the Birck Nanotechnology Center in Purdue University. This research was supported by NSF RAISE-TAQS Award No. 1839164. The CMP was completed at NOVASiC, and the AlN deposition was performed by Plasma-Therm.

DATA AVAILABILITY

The data that support the findings of this study are openly available in Zenodo at https://doi.org/10.5281/zenodo.4568410, Ref. 22.

REFERENCES

- ¹N. T. Son, C. P. Anderson, A. Bourassa, K. C. Miao, C. Babin, M. Widmann, M. Niethammer, J. Ul Hassan, N. Morioka, I. G. Ivanov, F. Kaiser, J. Wrachtrup, and D. D. Awschalom, "Developing silicon carbide for quantum spintronics," Appl. Phys. Lett. 116, 190501 (2020).
- ²S. J. Whiteley, G. Wolfowicz, C. P. Anderson, A. Bourassa, H. Ma, M. Ye, G. Koolstra, K. J. Satzinger, M. V. Holt, F. J. Heremans, A. N. Cleland, D. I. Schuster, G. Galli, and D. D. Awschalom, "Spin-phonon interactions in silicon carbide addressed by Gaussian acoustics," Nat. Phys. 15, 490-495 (2019).
- ³S. Gong, N. Kuo, and G. Piazza, "GHz high-Q lateral overmoded bulk acoustic-wave resonators using epitaxial SiC thin film," J. Microelectromech. Syst. 21, 253–255 (2012).
- ⁴A. L. Falk, B. B. Buckley, G. Calusine, W. F. Koehl, V. V. Dobrovitski, A. Politi, C. A. Zorman, P. X.-L. Feng, and D. D. Awschalom, "Polytype control of spin qubits in silicon carbide," Nat. Commun. 4, 1819 (2013).
- 5S. Castelletto, B. C. Johnson, V. Ivády, N. Stavrias, T. Umeda, A. Gali, and T. Ohshima, "A silicon carbide room-temperature single-photon source," Nat. Mater. 13, 151–156 (2014).
- ⁶I. Lekavicius, T. Oo, and H. Wang, "Diamond Lamb wave spin-mechanical resonators with optically coherent nitrogen vacancy centers," J. Appl. Phys. 126, 214301 (2019).
- ⁷B. Jiang, N. Opondo, G. Wolfowicz, P. Yu, D. D. Awschalom, and S. A. Bhave, "SiC cantilevers for generating uniaxial stress," in 2019 20th International Conference on Solid-State Sensors, Actuators and Microsystems Eurosensors XXXIII (TRANSDUCERS EUROSENSORS XXXIII) (2019), pp. 1655–1658.
- ⁸E. R. MacQuarrie, T. A. Gosavi, A. M. Moehle, N. R. Jungwirth, S. A. Bhave, and G. D. Fuchs, "Coherent control of a nitrogen-vacancy center spin ensemble with a diamond mechanical resonator," Optica 2, 233–238 (2015).
- ⁹B. P. Harrington and R. Abdolvand, "In-plane acoustic reflectors for reducing effective anchor loss in lateral-extensional MEMS resonators," J. Micromech. Microeng. 21, 085021 (2011).

- ¹⁰S. Maity, L. Shao, S. Bogdanović, S. Meesala, Y.-I. Sohn, N. Sinclair, B. Pingault, M. Chalupnik, C. Chia, L. Zheng, K. Lai, and M. Lončar, "Coherent acoustic control of a single silicon vacancy spin in diamond," Nat. Commun. 11, 193 (2020).
- ¹¹H. Chen, N. F. Opondo, B. Jiang, E. R. Macquarrie, R. S. Daveau, S. A. Bhave, and G. D. Fuchs, "Engineering electron-phonon coupling of quantum defects to a semiconfocal acoustic resonator," Nano Lett. 19, 7021–7027 (2019).
- ¹²L. Thiel, Z. Wang, M. A. Tschudin, D. Rohner, I. Gutiérrez-Lezama, N. Ubrig, M. Gibertini, E. Giannini, A. F. Morpurgo, and P. Maletinsky, "Probing magnetism in 2D materials at the nanoscale with single-spin microscopy," Science 364, 973–976 (2019).
- ¹³H. Mansoorzare, S. Moradian, S. Shahraini, R. Abdolvand, and J. Gonzales, "Achieving the intrinsic limit of quality factor in VHF extensional-mode block resonators," in 2018 IEEE International Frequency Control Symposium (IFCS) (2018), pp. 1–4.
- 14Y. Chinone, S. Ezaki, F. Fujita, and K. Matsumoto, Applications of High Purity SiC Prepared by Chemical Vapor Deposition BT - Amorphous and Crystalline Silicon Carbide II (Springer, Berlin/Heidelberg 1989), pp. 198–206.
- ¹⁵A. Kourani, R. Lu, and S. Gong, "A wideband oscillator exploiting multiple resonances in lithium niobate MEMS resonator," IEEE Trans. Ultrason., Ferroelectr., Frequency Control 67, 1854–1866 (2020).
- ¹⁶M. Ziaei-Moayyed, S. D. Habermehl, D. W. Branch, P. J. Clews, and R. H. Olsson, "Silicon carbide lateral overtone bulk acoustic resonator with ultrahigh quality factor," in Proceedings of the IEEE International Conference on Micro Electro Mechanical Systems (MEMS) (2011), pp. 788–792.
- ¹⁷V. Milanovic, M. Last, and K. S. J. Pister, "Laterally actuated torsional micromirrors for large static deflection," IEEE Photonics Technol. Lett. 15, 245–247 (2003)
- ¹⁸B. Hamelin, J. Yang, A. Daruwalla, H. Wen, and F. Ayazi, "Monocrystalline silicon carbide disk resonators on phononic crystals with ultra-low dissipation bulk acoustic wave modes," Sci. Rep. 9, 18698 (2019).
- ¹⁹V. J. Gokhale, B. P. Downey, D. S. Katzer, N. Nepal, A. C. Lang, R. M. Stroud, and D. J. Meyer, "Epitaxial bulk acoustic wave resonators as highly coherent multi-phonon sources for quantum acoustodynamics," Nat. Commun. 11, 2314 (2020).
- 20 D. M. Lukin, M. A. Guidry, and J. Vučković, "Integrated quantum photonics with silicon carbide: Challenges and prospects," PRX Quantum 1, 20102 (2020)
- ²¹J. Borysiuk, J. Sołtys, J. Piechota, S. Krukowski, J. M. Baranowski, and R. Stępniewski, "Structural defects in epitaxial graphene layers synthesized on C-terminated 4H-SiC (0001) surface-Transmission electron microscopy and density functional theory studies," J. Appl. Phys. 115, 054310 (2014).
- ²²B. Jiang, N. Opondo, and S. Bhave (2021). "Semi-insulating 4H-SiC lateral bulk acoustic wave resonators," Zenodo. https://doi.org/10.5281/zenodo.4568410